

Electronic Supplementary Information

The photocathodic properties of $\text{Pb}(\text{Zr}_{0.2}\text{Ti}_{0.8})\text{O}_3$ wrapped CaFe_2O_4 layer on ITO coated quartz for water splitting

Xiaorong Cheng, Deliang Chen, Wen Dong, Fengang Zheng, Liang Fang and Mingrong Shen*

Department of Physics & Jiangsu Key Laboratory of Thin Films & Collaborative Innovation Center of Suzhou Nano Science and Technology, Soochow University, Suzhou 215006, China. Email: mrshen@suda.edu.cn

S1 : Experimental Section

PCP film prepared by Sol-gel and EPD method: The CFO powder was synthesized by calcining the corresponding gel at 450°C for 2 hours and 1050°C for 10 hours as described in reference.¹ The PZT layers were firstly deposited on ITO quartz substrate by the sol-gel method. The PZT gel was prepared as described in our previous work.² Spin-coating was employed to deposit the PZT gel at about 1000 rpm for 5 seconds, then 3000 rpm for 25 seconds onto the ITO\quartz substrates. After the first spin-coating, the PZT film was dried at 150°C for 2 minutes and then put into oven where the samples are treated under 650°C for 2 hours in air. The first well crystallized PZT layer is formed on ITO\quartz substrates and the contact between ITO/PZT is expected. To exclude the direct contact of CFO with ITO, another 5 PZT layers were deposited at a lower spin speed of 1000 rpm for 25 seconds one by one. Then the film was dried at 150 °C. This amorphous PZT (a-PZT) also makes the whole film contact to the substrate tightly, as shown in Fig. 1d. The CFO layer was then deposited by EPD method in a constant voltage mode as described in reference.³ 40 mg CFO powder and 10 mg iodine were suspended in 50 ml acetone by ultrasonic concussion for 15 minutes. Two a-PZT/PZT/ITO substrates were immersed in the solution in parallel at a distance of 1cm and 50 V of voltage is applied between the substrates for 2 minutes by a DC power supply. When the CFO layer was dried in a 80°C oven, another 5 PZT layers were deposited on the CFO layer by the sol-gel method and dried at 150°C as well. After that the a-PZT\CFO\a-PZT samples were put into 650°C

oven to treat for 2 hours in air, to form a PZT wrapped CFO (PCP) layer on ITO coated quartz.

Ag nanoparticles fabricated by photoreduction method: The photoreduction of Ag nanoparticles on PCP film surface were carried out following the reference.⁴ A drop (approximately 0.2 ml) of 0.5 M AgNO₃ solution was placed onto the PCP film surface. Then the samples were irradiated with a 300 W Hg lamp for 20 minutes. After each period of photoreduction of Ag nanoparticles, the photocurrent was measured using an electrochemical workstation (CHI660D) with a 100 mW cm⁻² Xe lamp and 0.1 M Na₂SO₄ as electrolyte. After PEC measurements, the samples were again thoroughly rinsed with deionized water and dried in air. Another period of Ag particles growth was performed repeatedly. One obvious advantage of this procedure is that we can know how many periods for the deposition or photoreduction of Ag particles on PCP film is the best for the PEC performance of photocurrent.

Sample characterizations: The CFO powder and fabricated PCP films were characterized by Rigaku D/MAX 3C x-ray diffractometer (XRD) using Cu K α radiation. Scanning electron microscope (SEM) surface and cross-section images were checked by Hitachi SU8010. UV-Visible light absorption characteristic were measured by JASCO UV/VIS 550. The photocurrent and J-V curve of samples was measured by an electrochemical workstation (CHI660D) with a 100 mW cm⁻² Xe lamp as light source and 0.1 M Na₂SO₄ solution as electrolyte. During the measurement, the samples were illuminated by Xe lamp light source through bottom ITO substrate and served as working electrode, a Pt wire as the counter electrode and a Ag/AgCl electrode as the reference electrode. Potentiostatic electrochemical impedance spectroscopy (EIS) was carried with an AC potential frequency range from 100 000 to 0.1 Hz.

The measurement of H₂ and O₂ evolution: The hydrogen and oxygen evolution by PEC water splitting was conducted in the airtight photo-reactor which was made of quartz glass. In the photo-reactor, the photocathode and the counter electrode (Pt mesh) were separated in different tubular chambers, which avoid the mixing of hydrogen generated on the photocathode and oxygen on the Pt counter electrode. 1 M

HClO₄ solution was used as an electrolyte. The 100 mW cm⁻² Xe lamp was used as light source. The amount of hydrogen was determined by a gas chromatography equipped with TCD (Tianmei, GC 7890T).

S2: Photocurrent density of the CFO layer deposited on PZT/ITO by EPD method.

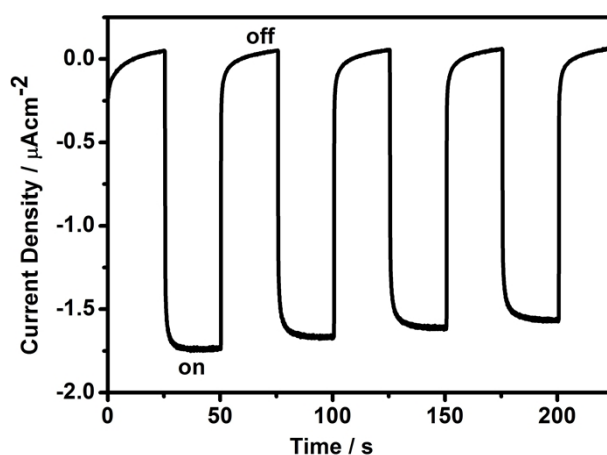


Fig. S1 Photocurrent density of the CFO layer deposited on PZT/ITO by EPD method. The photocurrent was measured with a 100 mW cm⁻² Xe lamp as light source and 0.1 M Na₂SO₄ solution as electrolyte. Without the PZT gel penetration the porous CFO layer is loosely contacted on the PZT/ITO/quartz substrates only by electrical field. The photocurrent was barely observed to be about 1.5 $\mu\text{A cm}^{-2}$.

S3: Photocurrent density of CFO layer deposited on PZT/ITO have either bottom (black) or top (red) 5-PZT-layer.

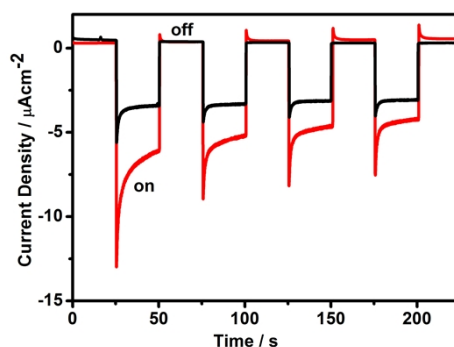


Fig. S2 Photocurrent density of CFO layer deposited on PZT/ITO have either bottom (black) or top (red) 5-PZT-layer measured with a 100 mW cm⁻² Xe lamp as light

source and 0.1 M Na_2SO_4 solution as electrolyte. The CFO layer deposited on PZT/ITO has bottom 5-PZT-layer show a small increased photocurrent of $3.7 \mu\text{A cm}^{-2}$ comparing with the CFO layer deposited on PZT/ITO by EPD method, which indicated that the bottom 5-PZT-layer enhanced the connection between the CFO layer and ITO/PZT substrate. The one has top 5-PZT-layer also exhibits a small increased photocurrent of about $5 \mu\text{A cm}^{-2}$, which can be contributed to the improvement of connection among CFO layer through PZT.

S4: EDX cross-section result of the prepared PCP layer.

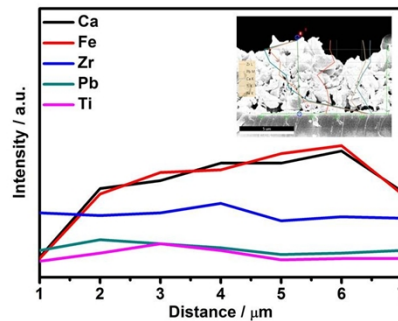


Fig. S3 EDX cross-section result of the prepared PCP layer. The EDX analysis confirms the PZT wrapped CaFe_2O_4 layer structure.

S5: Schematic models of (a) CFO layer deposited on PZT/ITO by EPD method and (b) PCP layer.

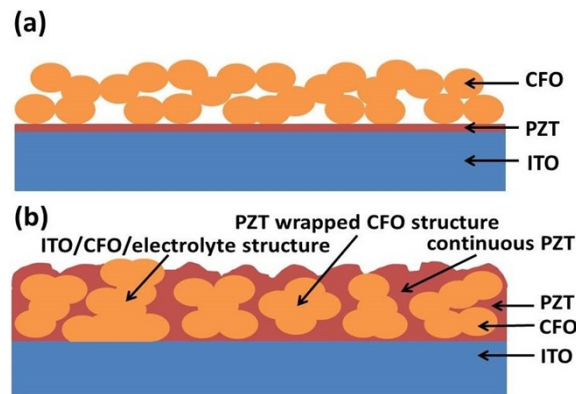


Fig. S4 Schematic models of (a) CFO layer deposited on PZT/ITO by EPD method and (b) PCP layer. The top and bottom PZT layers make the composite as a whole. In

Fig. S4b, we presented three main cases which may contribute to the photocathodic current of the PCP photoelectrode. One is the ITO/PZT/electrolyte junction resulting from continuous PZT film between electrolyte and ITO. The second is the PZT wrapped CFO structure (ITO/PZT/CFO/PZT/electrolyte) with PZT/CFO/PZT heterojunction. The third is that part of CFO is in direct contact with the solution while other part of CFO is in direct contact with ITO, forming a direct ITO/CFO/electrolyte photocathode because CFO is a p-type semiconductor. Based on the fabrication processes, where a crystallized PZT layer is pre-prepared on ITO and Ca and Fe elements decrease sharply on the film/ITO interface as shown in Figure S3, we proposed that the third case may not be the main structure responsible for the photocurrent in this study.

S6: XRD pattern of the CFO powder, PCP film and PCP film with the decoration of Ag.

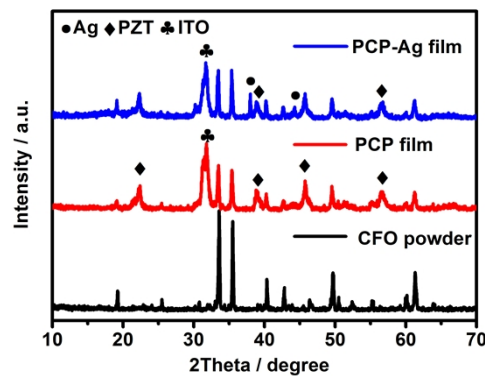


Fig. S5 XRD pattern of the CFO powder, PCP film and PCP film decorated by Ag. All the three parts are in their own phase, and no new phase are observed.

S7: Photocurrent under zero voltage vs. Ag/AgCl measured in a PEC cell for the PCP film and polarized and Ag decorated PCP film. Ag n refers to the n times of Ag photoreduction.

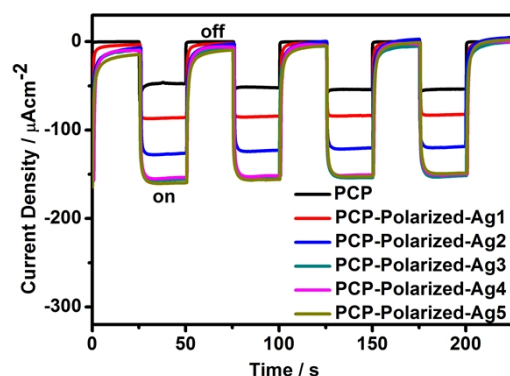


Fig. S6 Photocurrent under zero voltage vs. Ag/AgCl measured in a PEC cell for the PCP film and positively polarized PCP film with Ag decoration. The photocurrent was measured with a 100 mW cm^{-2} Xe lamp as light source and $0.1 \text{ M Na}_2\text{SO}_4$ solution as electrolyte. Ag n refer to the n times of Ag photoreduction. The photocurrent increases as the Ag photoreduction times increase from 1 to 3. Although there are small differences on the photocurrent during the repeated Ag deposition experiments, 3 times of Ag depositions always result in the best PEC performance, and the photocurrent reaches about $152 \text{ } \mu\text{A cm}^{-2}$.

S8: The solar-to-chemical conversion efficiency of poled and Ag decorated PCP film.

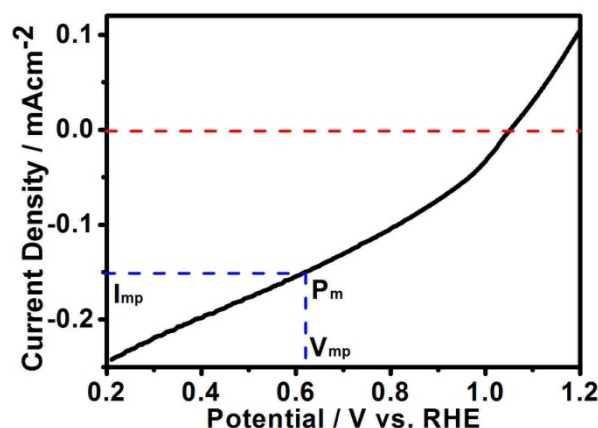


Fig. S7 The current – voltage behavior of polarized PCP film with Ag decoration carried out in $0.1 \text{ M Na}_2\text{SO}_4$ with the applied voltage versus RHE. Electrolyte ($\text{pH} = 7$) is a Ag/AgCl electrode as the reference electrode ($E_{\text{Ag}/\text{AgCl}} = 0.197\text{V}$). The potential is calculated based on $E_{\text{RHE}} = E + 0.059 \times \text{pH} + E_{\text{Ag}/\text{AgCl}}$. The solar-to-chemical conversion efficiency can be calculated from the current-voltage data by the following

equation: $\eta = J_{mp} V_{mp} / P_{in} \times 100\%$, where J_{mp} (mA) is the current density at the maximum power point (P_m), V_{mp} is the voltage vs. RHE at the P_m point, and P_{in} ($mW\ cm^{-2}$) is the power density of the incoming illumination.⁵ Here $J_{mp} = 0.15\ mA\ cm^{-2}$, $V_{mp} = 0.63\ V$, $P_{in} = 100\ mW\ cm^{-2}$. So the η is nearly 0.1% for polarized plus Ag decorated PCP film.

S9: The incident photo-to-current conversion efficiency (IPCE) spectra of poled and Ag decorated PCP film.

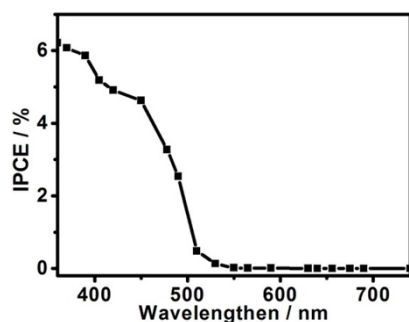


Fig. S8 The incident photo-to-current conversion efficiency (IPCE) for the positively polarized PCP film with Ag decoration measured in 0.1 M Na_2SO_4 solution. The IPCE value was calculated using the following equation: $IPCE\ (\%) = (1240 \times I / (\lambda \times J_{light})) \times 100\%$ where I is the photocurrent density ($mA\ cm^{-2}$), J_{light} is the power density of the incident illumination ($mW\ cm^{-2}$) and λ is the incident light wavelength (nm).

Looking back our previous study for ITO/PZT/Ag photocathode,⁶ the IPCE between 400 and 500 nm due to the presence of Ag nanoparticle is quite small comparing with the high IPCE in current Ag decorated PCP film. Therefore, the ITO/PZT/Ag junction resulting from continuous PZT film between Ag and ITO in this study is not the main reason for the obvious visible-light IPCE shown in Fig. S8. Instead, we proposed this is originated from the PZT wrapped CFO structure where CFO absorbs visible-light and the corresponding photocarriers can get out the PZT/CFO/PZT heterostructure as proposed in Fig. 4d.

S10: The SEM surface morphology of the poled and Ag decorated before and after water splitting reaction.

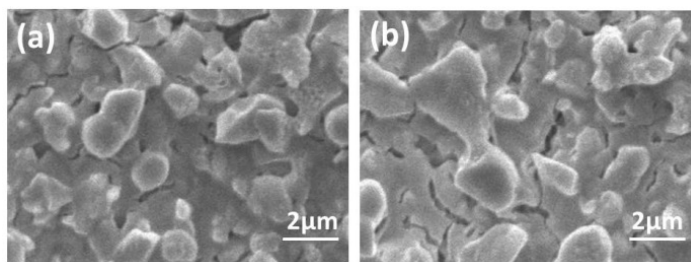


Fig. S9 The SEM surface morphology of the poled and Ag decorated PCP sample (a) before the water splitting reaction and (b) after 2 hours water splitting reaction. A as-grown sample was cut into two pieces. One was taken to SEM analysis directly and the other was taken to SEM analysis after water splitting reaction. There is no obvious corrosion on the film surface after water splitting reaction.

S11: The oxygen evolution of the poled and Ag decorated sample.



Fig. S10 The digital photo of the Pt counter electrode during the water splitting. Bubbles can be seen on the Pt counter electrode. The oxygen evolution of was measured under the exactly same condition as hydrogen evolution measurement. 1 M HClO_4 solution was used as an electrolyte and 100 mW cm^{-2} Xe lamp as light source. The evolved oxygen was determined by a gas chromatography equipped with TCD (Tianmei, GC 7890T). During the measurement, bubbles are clearly observed to evolve from the Pt counter electrode and confirmed by the GC measurements since the O_2 signal increases as time increases. However, because the small amount of oxygen exists in our home-made gas generation and collection system which can not be completely removed we are not able to determine the amount of evolved oxygen exactly at this moment. We will try to develop the appropriate method to do so in the future.

References:

- 1 Z.F. Liu, Z. G. Zhou and M. Miyouchi, *J. Phys. Chem. C*, Vol. **113**, No. 39, 2009.
- 2 C. Y. Wang, D. W. Cao, F. G. Zheng, W. Dong, L. Fang, X. D. Su and M. R. Shen, *Chem. Commun.*, 2013,**49**,3769.
- 3 E.S. Kim, N. Nishimaru, G. Magesh, J.Y. Kim, Ji-Wook Jang, H. Jun, J. Kubota, K. Domen and J. S. Lee, *J. Am. Chem. Soc.*, 2013, **135**, 5375.
- 4 M. Zhang, C. X. Jiang, W. Dong, F. G. Zheng, L. Fang, X. D. Su and M. R. Shen, *Appl. Phys. Lett.*, 2013,**103**,102902.
- 5 M.G. Walter, E.L. Warren, J.R. Mckone, S.W. Boettcher, Q.X. Mi, E.A. Santori and N.S. Lewis, *Chem. Rev.*, 2010,**110**,6446
- 6 C. Y. Wang, D. W. Cao, F. G. Zheng, W. Dong, L. Fang, X. D. Su and M. R. Shen, *Chem. Commun.*, 2013, **49**, 3769.